Electronic Supplementary Material (ESI) for Inorganic Chemistry Frontiers.

$Li_2CdGeSe_4$ and $Li_2CdSnSe_4$: Biaxial nonlinear optical materials with strong infrared second-order responses and laser-induced damage thresholds influenced by photoluminescence

Jian-Han Zhang,[a,b] Daniel J. Clark,[c] Ashley Weiland,[a] Stanislav, S. Stoyko,[a] Yong Soo Kim,[c] Joon I. Jang,[c] and Jennifer A. Aitken*[a]

Table S1. Atomic coordinates and equivalent isotropic displacement parameters ($Å^2 \times 10^3$) for$Li_2CdGeSe_4$ and $Li_2CdSnSe_4$.

Table S2. Selected bond lengths (Å) and angles (°) for $Li_2CdGeSe_4$ and $Li_2CdSnSe_4$.

Table S3. The unit cell parameters of $Li_2CdGeSe_4$ and $Li_2CdSnSe_4$ obtained from the Rietveld refinements using X-ray powder diffraction data.

Table S4. The bond length, corresponding bond valence and bond order of $Li_2CdGeSe_4$ and $Li_2CdSnSe_4$.

Table S5. State energies (eV) of the lowest conduction band (LCB) and the highest valence band (HVB) of the crystals of $Li_2CdGeSe_4$ and $Li_2CdSnSe_4$.

Figure S1 Differential thermal analysis diagrams for the heating (red)/cooling (blue) cycle of $Li_2CdSnSe_4$. The heating and cooling portions of the cycle are depicted in red and blue, respectively.

Figure S2. X-ray powder diffraction patterns for $Li_2CdGeSe_4$ and $Li_2CdSnSe_4$ before and after DTA compared to the calculated pattern.

Figure S3 Optical diffuse reflectance UV/vis/NIR spectral data converted to absorption for $Li_2CdGeSe_4$ (left) and $Li_2CdSnSe_4$ (right). Data were obtained for fresh (solid line) samples and the same samples exposed to ambient conditions for one week (dotted line). The signficiant difference in the observed optical bandgaps is attrributed to surface degredation due to air and/or moisture exposure.

Figure S4. SHG particle-size dependence of $Li_2CdGeSe_4$ at various wavelengths to determine the phase-matching onsets.

Figure S5. SHG particle-size dependence of $Li_2CdSnSe_4$ at various wavelengths to determine the phase-matching onsets.

Table S1. Atomic coordinates and equivalent isotropic displacement parameters ($Å^2 \times 10^3$) for $Li_2CdGeSe_4$ and $Li_2CdSnSe_4$.

Atom	x	y	z	U(eq)
$Li_2CdGeSe_4$				
Li(1)	1.0758(5)	0.2434(8)	0.094(2)	0.028(2)
Li(2)	0.8401(5)	-0.0031(8)	0.073(5)	0.025(2)
Cd(1)	0.6600(2)	0.0070(1)	0.5815(2)	0.021(1)
Ge(1)	0.9117(1)	0.2533(1)	0.5833(1)	0.013(1)
Se(1)	0.8344(1)	0.4896(1)	0.6865(1)	0.017(1)
Se(2)	1.0665(1)	0.2409(1)	0.7090(1)	0.017(1)
Se(3)	0.9103(1)	0.2427(1)	0.2322(1)	0.017(1)
Se(4)	0.8375(1)	0.0194(1)	0.7051(1)	0.017(2)
$Li_2CdSnSe_4$				
Li(1)	0.1603(6)	0.505(1)	0.254(6)	0
Li(2)	0.0748(7)	-0.260(1)	0.746 (4)	0
Cd(1)	0.1634 (1)	-0.0044(1)	0.2481 (3)	0.025(1)
Sn(1)	0.4140(1)	-0.2526(1)	0.2498(2)	0.014(1)
Se(1)	0.0768(1)	-0.2526(1)	0.2498(2)	0.019(1)
Se(2)	0.0875(1)	0.2570(1)	0.3803(1)	0.019(1)
Se(3)	0.1683(1)	-0.0007(1)	-0.1403(1)	0.018(1)
Se(4)	0.3359(1)	0.0053(1)	0.3761(1)	0.017(1)

Table S2. Selected bond lengths (Å) and angles (°) for$Li_2CdGeSe_4$ and $Li_2CdSnSe_4$.[a]

$Li_2ZnGeSe_4$			
Li(1)-Se(3)	2.517(7)	Li(1)-Se(2)#1	2.574(13)
Li(1)-Se(4)#2	2.612(7)	Li(1)-Se(1)#3	2.630(7)
Li(2)-Se(4)#1	2.46(4)	Li(2)-Se(3)	2.508(16)
Li(2)-Se(2)#2	2.545(13)	Li(2)-Se(1)#4	2.583(13)
Cd(1)-Se(3)#5	2.6115(6)	Cd(1)-Se(2)#6	2.6188(7)
Cd(1)-Se(1)#4	2.6443(12)	Cd(1)-Se(4)	2.6445(5)
Ge(1)-Se(2)	2.3473(5)	Ge(1)-Se(3)	2.3473(6)
Ge(1)-Se(1)	2.3490(5)	Ge(1)-Se(4)	2.3525(5)
Se(3)-Li(1)-Se(2)#1	108.6(4)	Se(3)-Li(1)-Se(4)#2	109.3(3)
Se(2)#1-Li(1)-Se(4)#2	107.6(3)	Se(3)-Li(1)-Se(1)#3	111.4(3)
Se(2)#1-Li(1)-Se(1)#3	105.5(3)	Se(4)#2-Li(1)-Se(1)#3	114.3(3)
Se(4)#1-Li(2)-Se(3)	111.6(7)	Se(4)#1-Li(2)-Se(2)#2	115.0(8)
Se(3)-Li(2)-Se(2)#2	105.9(8)	Se(4)#1-Li(2)-Se(1)#4	106.3(7)
Se(3)-Li(2)-Se(1)#4	105.8(8)	Se(2)#2-Li(2)-Se(1)#4	111.9(8)
Se(3)#5-Cd(1)-Se(2)#6	110.75(3)	Se(3)#5-Cd(1)-Se(1)#4	110.49(3)
Se(2)#6-Cd(1)-Se(1)#4	112.54(3)	Se(3)#5-Cd(1)-Se(4)	105.90(3)
Se(2)#6-Cd(1)-Se(4)	110.30(3)	Se(1)#4-Cd(1)-Se(4)	106.58(3)
Se(2)-Ge(1)-Se(3)	111.31(2)	Se(2)-Ge(1)-Se(1)	111.449(19)
Se(3)-Ge(1)-Se(1)	108.70(2)	Se(2)-Ge(1)-Se(4)	104.833(18)
Se(3)-Ge(1)-Se(4)	108.11(2)	Se(1)-Ge(1)-Se(4)	112.38(2)
$Li_2CdSnSe_4$			
Li(1)-Se(1)#1	2.476(17)	Li(1)-Se(2)	2.489(18)
Li(1)-Se(4)#2	2.57(4)	Li(1)-Se(3)#3	2.580(16)
Li(2)-Se(1)	2.49(3)	Li(2)-Se(2)#4	2.517(13)
Li(2)-Se(4)#5	2.587(13)	Li(2)-Se(3)#6	2.678(12)
Cd(1)-Se(2)	2.6136(14)	Cd(1)-Se(1)	2.6276(15)
Cd(1)-Se(4)	2.6410(12)	Cd(1)-Se(3)	2.643(3)

Sn(1)-Se(3)#5	2.5130(11)	Sn(1)-Se(1)#7	2.5140(11)
Sn(1)-Se(2)#8	2.5153(17)	Sn(1)-Se(4)	2.5154(11)
Se(1)#1-Li(1)-Se(2)	110.3(10)	Se(1)#1-Li(1)-Se(4)#2	112.5(11)
Se(2)-Li(1)-Se(4)#2	108.9(10)	Se(1)#1-Li(1)-Se(3)#3	112.8(10)
Se(2)-Li(1)-Se(3)#3	107.0(9)	Se(4)#2-Li(1)-Se(3)#3	104.9(9)
Se(1)-Li(2)-Se(2)#4	111.9(6)	Se(1)-Li(2)-Se(4)#5	110.0(6)
Se(2)#4-Li(2)-Se(4)#5	110.4(7)	Se(1)-Li(2)-Se(3)#6	106.1(6)
Se(2)#4-Li(2)-Se(3)#6	110.9(6)	Se(4)#5-Li(2)-Se(3)#6	107.3(6)
Se(2)-Cd(1)-Se(1)	111.36(7)	Se(2)-Cd(1)-Se(4)	106.54(6)
Se(1)-Cd(1)-Se(4)	109.58(6)	Se(2)-Cd(1)-Se(3)	110.19(7)
Se(1)-Cd(1)-Se(3)	111.27(7)	Se(4)-Cd(1)-Se(3)	107.72(5)
Se(3)#5-Sn(1)-Se(1)#7	111.57(5)	Se(3)#5-Sn(1)-Se(2)#8	108.66(5)
Se(1)#7-Sn(1)-Se(2)#8	111.00(4)	Se(3)#5-Sn(1)-Se(4	111.76(5)
Se(1)#7-Sn(1)-Se(4)	105.69(4)	Se(2)#8-Sn(1)-Se(4)	108.11(5)

[a] Symmetry transformations used to generate equivalent atoms:

For $Li_2CdGeSe_4$: #1 x,y,z-1; #2 -x+2,-y,z-1/2; #3 -x+2,-y+1,z-1/2; #4 -x+3/2,y-1/2,z-1/2; #5 -x+3/2,y-1/2,z+1/2; #6 x-1/2,-y+1/2,z.

For $Li_2CdSnSe_4$: #1 x,y+1,z; #2 -x+1/2,y+1/2,z-1/2; #3 -x+1/2,y+1/2,z+1/2; #4 -x,-y,z+1/2; #5 -x+1/2,y-1/2,z+1/2; #6 x,y,z+1; #7 x+1/2,-y-1/2,z; #8 -x+1/2,y-1/2,z-1/2.

Table S3. The unit cell parameters of $Li_2CdGeSe_4$ and $Li_2CdSnSe_4$ obtained from the Rietveld refinements using X-ray powder diffraction data.

	$Li_2CdGeSe_4$	$Li_2CdSnSe_4$
Space group	*Pna*2$_1$	*Pna*2$_1$
a (Å)	14.1477(2)	14.4688(6)
b (Å)	8.3027(1)	8.4152(3)
c (Å)	6.67935(8)	6.81134(2)
V (Å^3)	784.58(1)	829.34(5)

Table S4. The bond length, corresponding bond valence and bond order of $Li_2CdGeSe_4$ and $Li_2CdSnSe_4$.

Bond	Bond length(Å)	Bond valence	Bond order
$Li_2CdGeSe_4$			
Li(1)-Se(1)	2.630(7)	0.22	0.21
Li(1)-Se(2)	2.574(13)	0.25	0.05
Li(1)-Se(3)	2.517(7)	0.30	0.04
Li(1)-Se(4)	2.612(7)	0.23	0.18
	ΣBV=	1.00	
Li(2)-Se(1)	2.583(13)	0.25	0.22
Li(2)-Se(2)	2.545(13)	0.27	0.12
Li(2)-Se(3)	2.508(16)	0.30	0.16
Li(2)-Se(4)	2.46(4)	0.34	0.08
	ΣBV=	1.16	
Cd(1)-Se(1)	2.6443(12)	0.49	0.60
Cd(1)-Se(2)	2.6188(7)	0.53	1.00
Cd(1)-Se(3)	2.6115(6)	0.54	1.03
Cd(1)-Se(4)	2.6445(5)	0.49	0.59
	ΣBV=	2.05	
Ge(1)-Se(1)	2.3490(5)	1.00	1.48
Ge(1)-Se(2)	2.3473(5)	1.00	1.52
Ge(1)-Se(3)	2.3473(6)	1.00	1.49
Ge(1)-Se(4)	2.3525(5)	0.99	1.31
	ΣBV=	3.99	
$Li_2CdSnSe_4$			
Li(1)-Se(1)	2.476(17)	0.33	-1.55
Li(1)-Se(2)	2.489(18)	0.32	-0.38
Li(1)-Se(3)	2.580(16)	0.25	-1.27
Li(1)-Se(4)	2.57(4)	0.25	0.00

	ΣBV=	1.15	
Li(2)-Se(1)	2.49(3)	0.32	-0.12
Li(2)-Se(2)	2.517(13)	0.30	-0.32
Li(2)-Se(3)	2.678(12)	0.19	-0.50
Li(2)-Se(4)	2.587(13)	0.24	-0.70
	ΣBV=	1.05	
Cd(1)-Se(1)	2.6276(15)	0.52	1.22
Cd(1)-Se(2)	2.6136(14)	0.54	1.13
Cd(1)-Se(3)	2.643(3)	0.50	1.13
Cd(1)-Se(4)	2.6410(12)	0.50	1.05
	ΣBV=	2.06	
Sn(1)-Se(1)	2.5140(11)	1.03	1.26
Sn(1)-Se(2)	2.5153(17)	1.03	1.16
Sn(1)-Se(3)	2.5130(11)	1.03	1.16
Sn(1)-Se(4)	2.5154(11)	1.03	0.99
	ΣBV=	4.12	

The bond valence calculation is based on Brown I. D.'s reference in 1985.[1]

$$V = \Sigma v_i = \Sigma \exp\left(\frac{r_0 - r}{0.37}\right) \qquad (1)$$

$$r_0 = r_c + A r_a + P - D - F \qquad (2)$$

In equation (1),V is the valence of cations, v_i is the bond valence, r_0 is a bond-valence parameter for certain bond, and r is the bond length. In equation (2), $r_c$and$r_a$are radii of cation and anion which can be foundin the tables of this reference,P, D and $F$are corrections required when the cation contains non-bonding *p*, *d*, and *f* electrons, respectively.

Bond order data is calculated by CASTEP program, where the structure used is without any volume or geometry optimization and the distance cut-off for Mulliken bond population analysis is set as 3.5 Å.

Table S5. State energies (eV) of the lowest conduction band (LCB) and the highest valence band (HVB) of the crystals of $Li_2CdGeSe_4$ and $Li_2CdSnSe_4$.

Formular	k-point	LCB	HVB
$Li_2CdGeSe_4$	G (0, 0, 0)	1.98235	0
	Z (0, 0, 0.5)	2.20005	-0.1922
	T (-0.5, 0, 0.5)	2.2554	-0.28422
	Y(-0.5, 0, 0)	2.32889	-0.07503
	S (-0.5, 0.5, 0)	2.72111	-0.19561
	X (0, 0.5, 0)	2.75768	-0.25945
	U (0, 0.5, 0.5)	2.60307	-0.34237
	R (-0.5, 0.5, 0.5)	2.57771	-0.34958
$Li_2CdSnSe_4$	G (0, 0, 0)	2.11426	0
	Z (0, 0, 0.5)	2.51946	-0.25508
	T (-0.5, 0, 0.5)	2.57844	-0.36792
	Y(-0.5, 0, 0)	2.45053	-0.08657
	S (-0.5, 0.5, 0)	2.92011	-0.23441
	X (0, 0.5, 0)	2.92011	-0.24567
	U (0, 0.5, 0.5)	2.92764	-0.49368
	R (-0.5, 0.5, 0.5)	2.90887	-0.48333

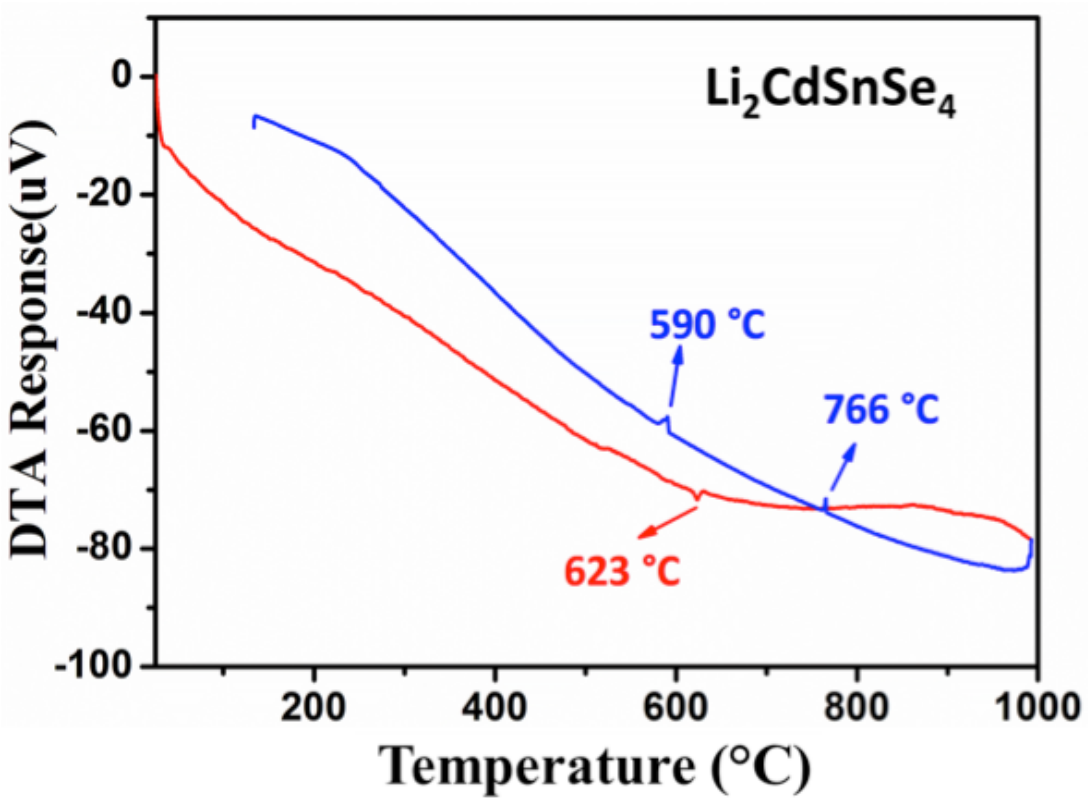

Figure S1. Differential thermal analysis diagrams for the heating (red)/cooling (blue) cycle of $Li_2CdSnSe_4$. The heating and cooling portions of the cycle are depicted in red and blue, respectively.

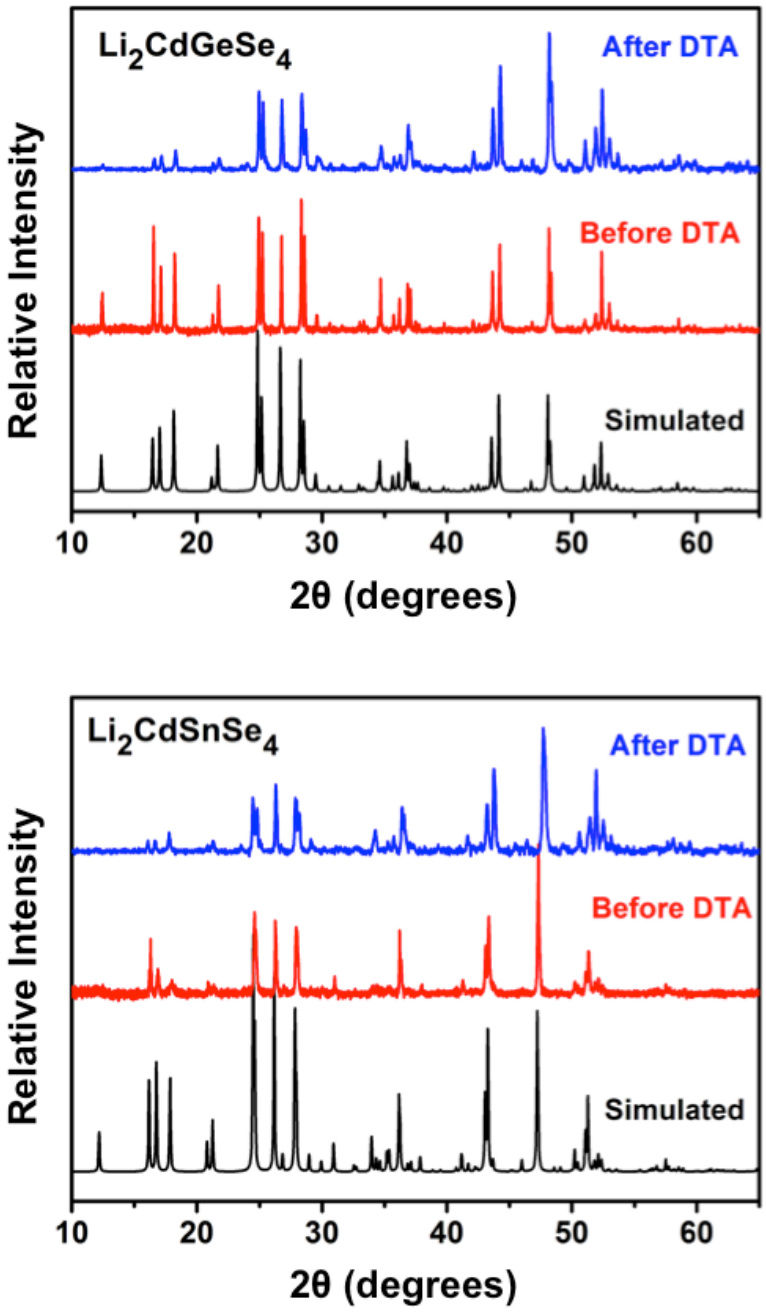

Figure S2. X-ray powder diffraction patterns for $Li_2CdGeSe_4$ and $Li_2CdSnSe_4$ before and after DTA compared to the calculated pattern.

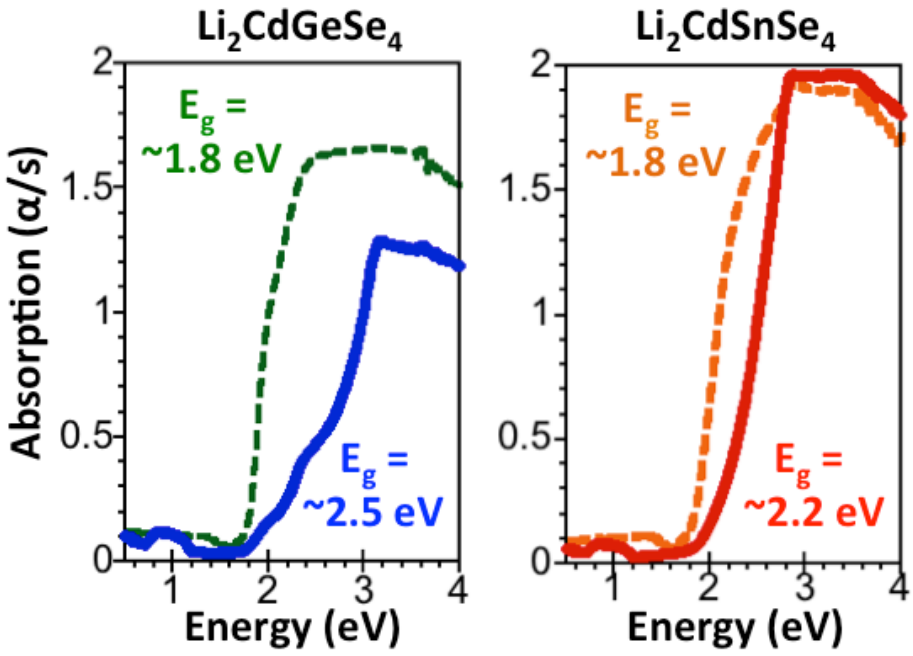

Figure S3. Optical diffuse reflectance UV/vis/NIR spectral data converted to absorption for $Li_2CdGeSe_4$ (left) and $Li_2CdSnSe_4$ (right). Data were obtained for fresh (solid line) samples and the same samples exposed to ambient conditions for one week (dotted line). The signficiant difference in the observed optical bandgaps is attrributed to surface degredation due to air and/or moisture exposure.

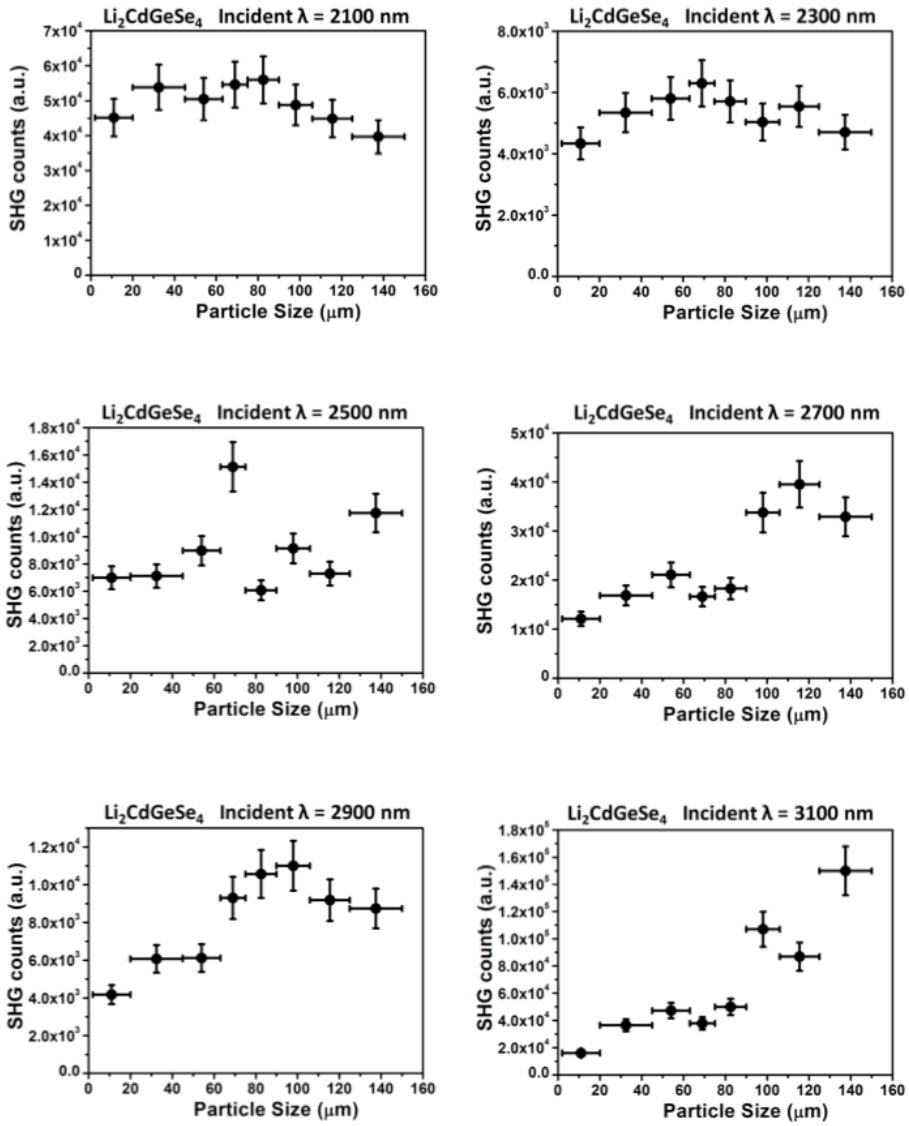

Figure S4. SHG particle-size dependence of $Li_2CdGeSe_4$ at various wavelengths to determine the phase-matching onsets.

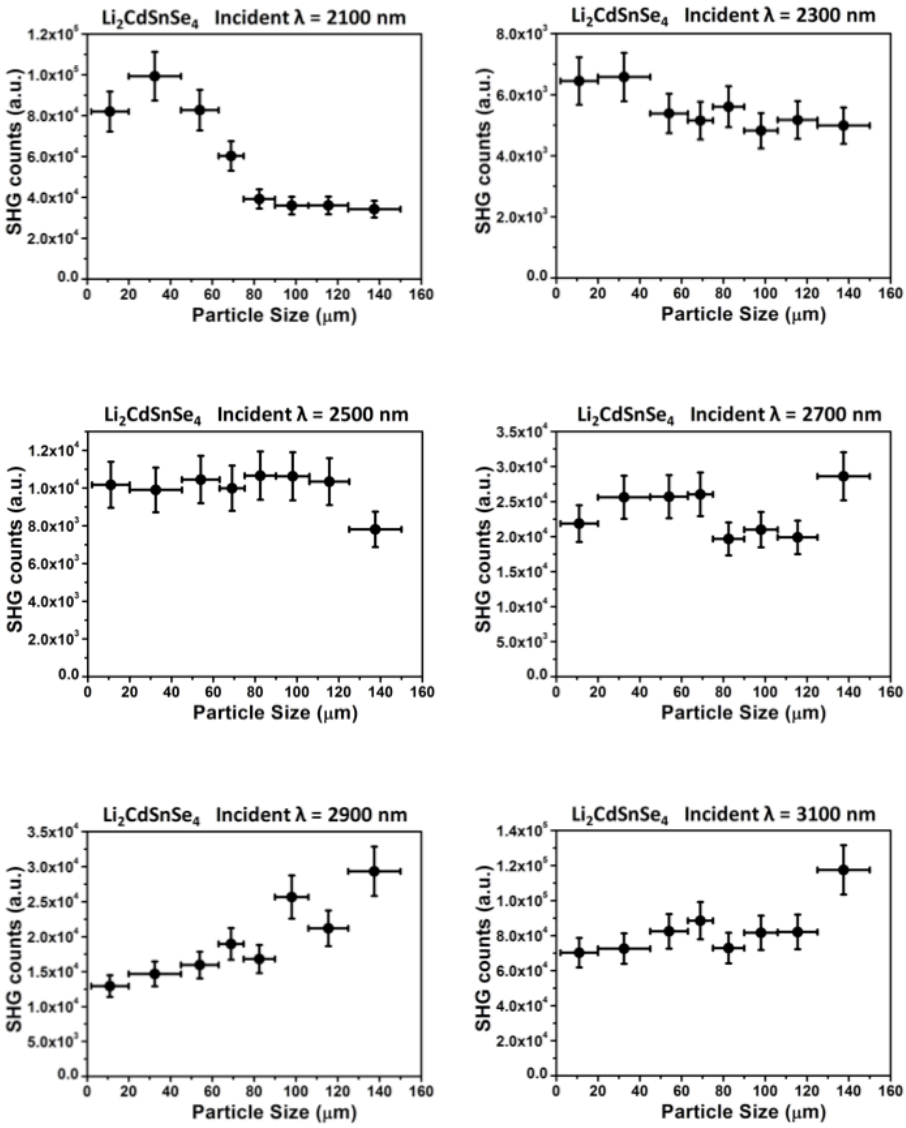

Figure S5. SHG particle-size dependence of $Li_2CdSnSe_4$ at various wavelengths to determine the phase-matching onsets.

1 I. D. Brown, D.Altermatt, *Acta, Cryst.*1985, **B41**, 244.